

Supporting Information

PtPd Nanoframes Derived from Pd@PdPt Core-Shell Rhombic Dodecahedrals with Excellent Catalytic Performance toward Methanol Oxidation

Yangyang Ren, Chuanliang Li, Baosong Li, Fan Gao, Xinghua Zhang, Xiaojing Yang, Lanlan Li,
Zunming Lu, Xiaofei Yu*

Determination of d-band center.

The d-band centers are obtained from the XPS valence band spectrum and the data ranging from 0 to -9 eV are imported into XPS peak software to create a baseline. Then, the d-band centers are calculated by the following equation:

$$\int N(\epsilon)\epsilon d\epsilon / \int N(\epsilon) d\epsilon$$

where $N(\epsilon)$ is the density of states (i. e. the photoelectron intensity after subtracting the background).²⁹

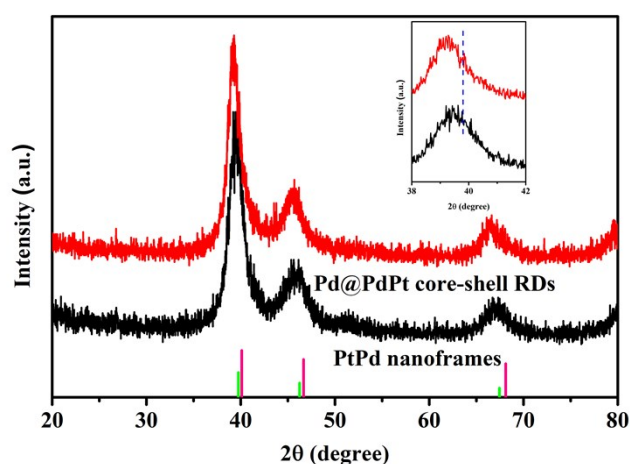


Fig. S1 XRD patterns of Pd@PdPt core-shell RDs and PtPd nanoframes. The inset shows the clear shift of the (111) peaks of Pd@PdPt core-shell RDs and PtPd nanoframes. Besides, the peak of PtPd nanoframes has a positive shift compared with that of Pd@PdPt core-shell RDs.

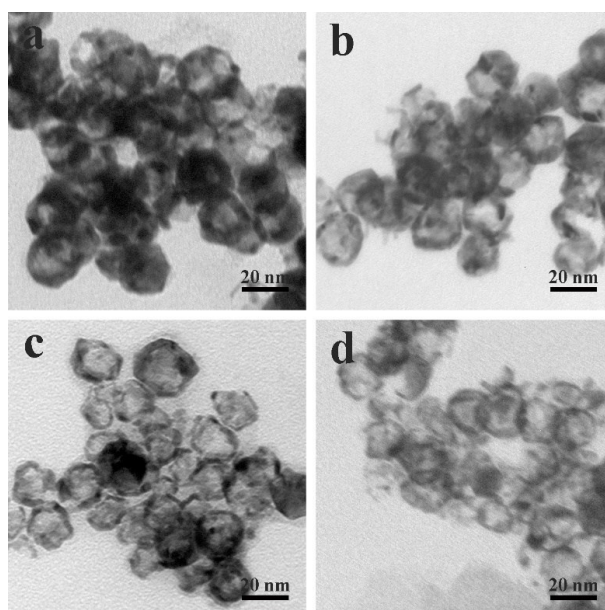


Fig. S2 TEM images obtained with different use of $\text{FeCl}_3 \cdot 6\text{H}_2\text{O}$: (a) 20 mg; (b) 35 mg; (c) 65 mg and (d) 80 mg.

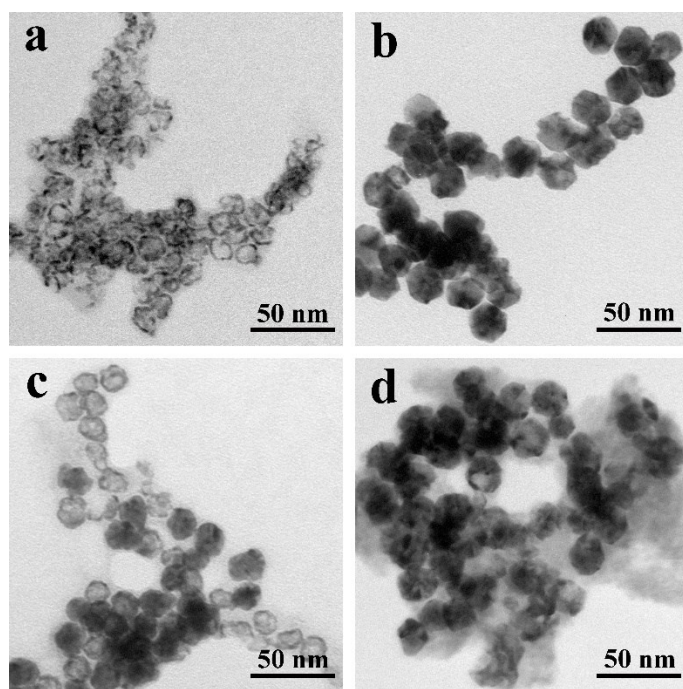


Fig. S3 TEM images obtained with different etching agents: (a) $\text{FeCl}_3 \cdot 6\text{H}_2\text{O} + \text{HNO}_3$; (b) $\text{ZnCl}_2 + \text{HCl}$; (c) $\text{Fe}(\text{NO}_3)_3 \cdot 9\text{H}_2\text{O} + \text{HCl}$ and (d) $\text{FeCl}_3 \cdot 6\text{H}_2\text{O}$.

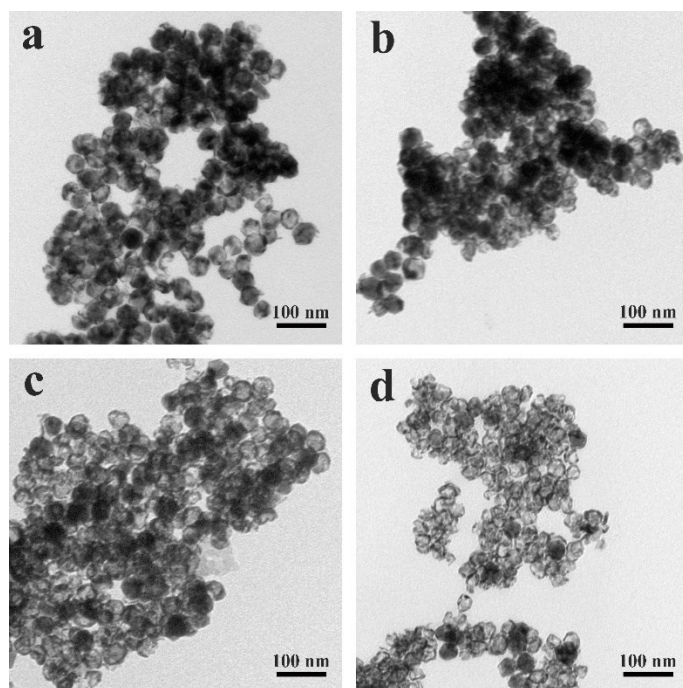


Fig. S4 TEM images obtained at different etching time: (a) 0.5 h; (b) 1 h; (c) 1.5 h and (d) 2 h.

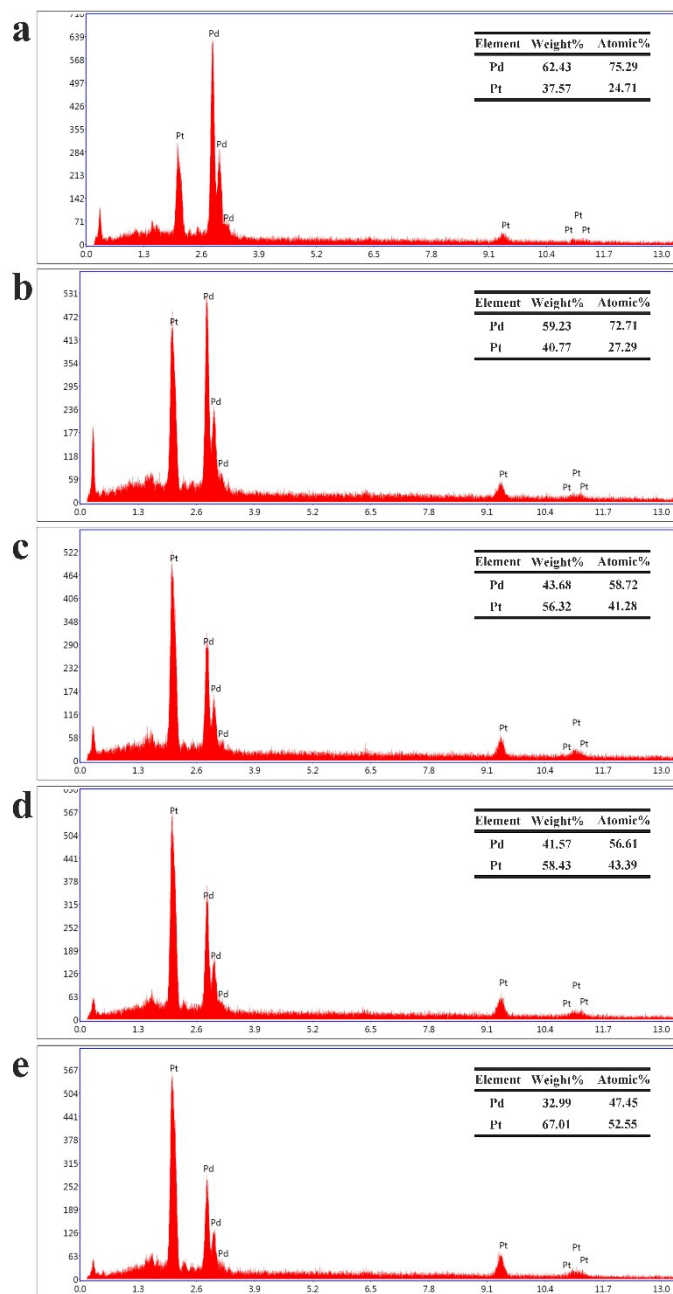


Fig. S5 EDS results obtained at different etching time: (a) 0 h; (b) 0.5 h; (c) 1 h; (d) 1.5 h and (e) 2 h.

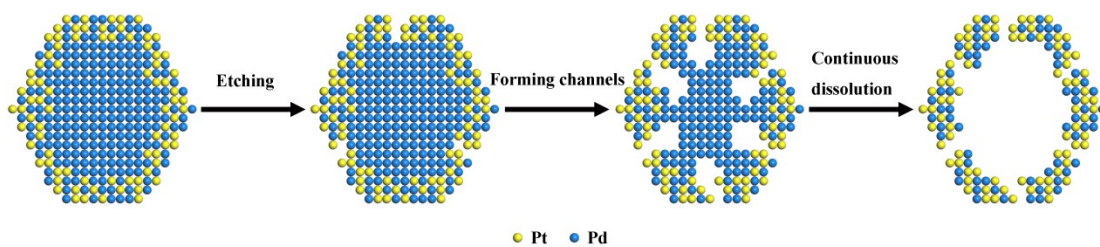


Fig. S6 The formation mechanism of PtPd nanoframes.

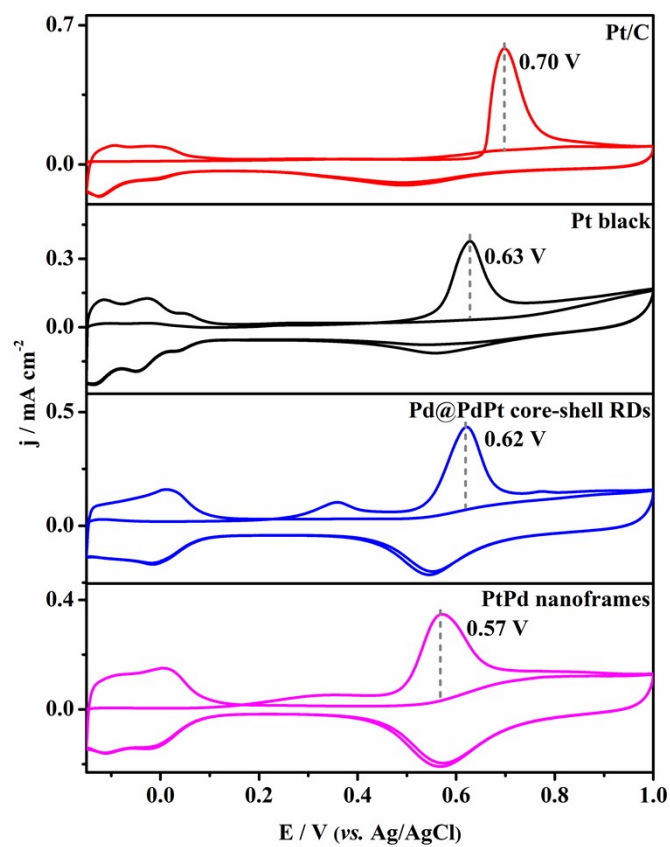


Fig. S7 CO-stripping curves of Pt/C, Pt black, Pd@PdPt core-shell RDs and PtPd nanoframes in 0.5 M H₂SO₄.